Indonesian Journal of Chemical Research

http://ojs3.unpatti.ac.id/index.php/ijcr Indo. J. Chem. Res., 12 (3), 213-219, 2025

Hydrothermal Synthesis and Characterization of Sodalite from Feldspar Mesawa Minerals

Ida Ifdaliah Amin[1,2*], Abdul Wahid Wahab[3], Paulina Taba[3], Rino R. Mukti[4], Giovanno Alvin S[4], Bulkis Musa[3], Hijrah A. Azis[2]

[1]Department of Technological of Metallurgy Extraction, Faculty of Vocational, Universitas Hasanuddin, Makassar City, South Sulawesi-Indonesia
[2]Department of Chemistry, Faculty of Engineering, Universitas Teknologi Sulawesi, Makassar City, South Sulawesi-Indonesia
[3]Department of Chemistry, Faculty Mathematics and Natural Science, Universitas Hasanuddin, South Sulawesi-Indonesia
[4]Division of Inorganic and Physical Chemistry, Institut Teknologi Bandung, Indonesia
[*]*Corresponding Author: idaifdaliah@unhas.ac.id*

Received: September 2024
Received in revised: January 2025
Accepted: January 2025
Available online: January 2025

Abstract

The mineral feldspar is a potential raw material in zeolite synthesis because of the high content of SiO_2 and Al_2O_3. Characterization of X-ray diffraction (XRD) and X-ray fluorescence (XRF) on Mesawa feldspar minerals showed high crystallinity and aluminosilicate composition. The synthesis of sodalite-type zeolite from Mesawa feldspar mineral has been successfully carried out. This research aims to investigate NaOH concentration's effect on changes in feldspar's structure. The feldspar mineral was prepared and then milled to pass through a 200-mesh sieve. The synthesis process uses the hydrothermal method with various times and concentrations of NaOH. The sample was mixed with NaOH, stirred until homogeneous at 300 rpm for 1 hour, and transferred to an autoclave. The autoclave was tightly closed and heated in an oven at 170 °C for 72 hours. XRD and XRF analysis revealed that the feldspar mineral had changed to sodalite with a purity of 90.89% and 90.06%; with a yield of 80.89% and 87.36%. FTIR characteristics show a specific peak for sodalite at 422-460 cm^{-1} related to Si-O bond vibrations, and absorption bands at 698 and 719 cm^{-1} related to Al-OH vibrations. The SEM results confirmed the morphology of the sodalite resembling balls like raspberries". This research proves that the Mesawa feldspar mineral sample contains type 6 secondary building units, the same blocks as zeolite analcime and cancrinite, so it has the potential as an adsorbent for heavy metals and as a catalyst alternative.

Keywords: Feldspar, hydrothermal, zeolite, sodalite, recrystallization

INTRODUCTION

Zeolite is a porous aluminosilicate crystal material having a size ranging from 0.5-1.2 nm with the formula M2/nO.Al2O3.ySiO2.wH2O, where M represents a metal cation, y=2-200, n represents the valence cation, and w represents the water content of the zeolite. The zeolite framework structure consists of tetrahedral [SiO4]4- dan [AlO4]5- (Kumar et al., 2022). The oxygen ions within the zeolite framework structure link between the SiO4 and AlO4 structures. In the zeolite framework, each tetrahedral AlO4 carries a negative charge from a cation. Ion exchange allows cations to move from one location to another (Flanigen et al., 2010).

Sodalite is a type of zeolite with a small pore size of 2.8 Å, characterized by a framework structure comprised of six rings. The framework structure of sodalite is cubic, consisting of β-cages. Each β-cage consists of 24 T atoms (T=Si4+ or Al3+) arranged in a tetrahedral configuration of SiO4 and AlO4 (An et al., 2020). The β-cages are interconnected by simple T4 rings, forming the overall framework structure of sodalite (Xu et al., 2009).

Zeolites are commonly classified into two groups: natural zeolites and synthetic zeolites. The formation of natural zeolites is a result of a complex chemical and physical process that occurs in rocks undergoing various transformations in a natural setting uch as clinoptololite and mordenite (Ngapa and Ika, 2020; Santoso et al., 2024). The composition of natural zeolites may vary. However, silica and alumina are the principal components. Additionally, natural zeolites contain minor elements such as Na, K, Ca, Mg, and Fe (Akimkhan, 2012). Despite their lower cost and wide availability, natural zeolites also have certain disadvantages, including the presence of impurities, which can have a negative impact on their

efficacy (Jiang et al., 2012). One potential solution to improving the effectiveness of natural zeolites is through recrystallization, activation, and modification processes (Kuznetsov et al., 2021; Perez-Botella et al., 2022).

Synthetic zeolites differ from natural ones in that they are engineered to exhibit desired zeolite characteristics suitable for their intended use. The basic principle of synthetic zeolite synthesis involves using raw materials, namely silica, and alumina, as the source of zeolite components to synthesize a specific type of zeolite with a defined composition. As a result, synthetic zeolites exhibit higher purity compared to natural zeolites. Research into the development of synthetic zeolites is currently focused on two main areas: raw materials and methods. Popular raw materials for zeolite development include coal fly ash (Klima et al., 2022; Luo et al., 2016), rice husk ash (Flores et al., 2021; Hamidi et al., 2021), and kaolin(Song et al., 2020); Oil palm shell ash (Fricha et al., 2024).

Prior research predominantly utilized synthetic zeolite, which necessitates a costly production process. The utilization of natural zeolite may mitigate synthesis expenses due to its abundance in Indonesia. Zeolite is distributed throughout the provinces of West Java, Lampung, East Nusa Tenggara, South Sulawesi, and North Sumatra in Indonesia (Kusdarto, 2008 in Setiawan et al., 2022). Zeolite is distributed in the Sangkaropi region of Tanah Toraja and the Seppong area of Majene, South Sulawesi (Kartawa et al., 2009 in Setiawa et al., 2022). The lack of utilization of natural resources originating from the West Sulawesi region, especially Mesawa, so in this study will use natural zeolite originating from Mesawa.

Feldspar is an aluminosilicate crystal with a general formula of M1+/M2+(AlSi)4O8, commonly written as MT4O8, where T is the abbreviation of the coordinating element with oxygen. M1+ dan M2+ represent the alkali or alkaline earth metals, acting as cation exchange agents (Pakhomova et al., 2020). The crystal lattice of feldspars has a three-dimensional framework with voids within formed by tetrahedral silica and alumina bound by oxygen atoms naturally (Wu et al., 2022; Ma et al., 2017). The composition of pure K-feldspar (KAlSi3O8) is 18 wt% Al2O3 and 16.9 wt% K2O (Salimkhani et al., 2020). This structure allows for feldspar to be modified in accordance with its intended application.

Synthesis of zeolites from feldspar can be achieved by adding compounds that produce strong polymer bonds. Researchers who have studied the production of zeolites from feldspar include (Su et al., 2016), who synthesized zeolite A from K-feldspar. The hydrothermal process is the most commonly used method for synthesizing zeolites from feldspar, where feldspar is mixed with an alkali solution at varying temperatures, pressures, and reaction times (Amin et al., 2023; He et al., 2016). The aim of this research is to re-crystallize and synthesize sodalite (SOD) from feldspar using the hydrothermal method. The samples produced in this research were characterized using Fourier Transform Infrared (FTIR), X-ray Diffraction (XRD), and Scanning Electron Microscopy (SEM). This research is expected to contribute to the utilization of feldspar and its potential benefits, such as optimizing its applications as a heterogeneous catalyst or an adsorbent for heavy metals in the environment, will be further understood through the characterization of the obtained zeolite.

This section should present the background of the research conducted, other studies that support (Spellman, 2013), this research is conducted which is new from the research conducted. The use of cited literature (Sutapa, Rosmawaty, & Samual, 2013), does not include literature that is not in the bibliography. It is not permitted to display figures and tables in this section (Bandjar, Sutapa, Rosmawaty, & Mahulau, 2014; Diop, Ben Talouba, Balland, & Mouhab, 2019; Sutapa et al., 2013).

METHODOLOGY

Materials and Instrumentals

Feldspar samples (milled to pass a 200 mesh sieve) were obtained from Mesawa village, West Sulawesi Province, Indonesia. Amin et al. 2023 presented evidence in the journal confirming that this sample is feldspar, Sodium hydroxide (NaOH) pa (as pellets 99%, Merck), and distilled water. Anhydrous sodium aluminosilicate ($NaAl_2O_3$) (Aldrich, Na_2O 4045%, Al_2O_3 50-56%).

Methods

The recrystallization procedure was executed utilizing hydrothermal, which excluded the activation steps and utilization of organic templates. The experiment began by preparing a sodium hydroxide (NaOH) solution by dissolving 3.6925 g of NaOH in 18 g of water.

The feldspar sample (0.8677 g) was then added to the solution and stirred until homogeneity. The mixture was transferred to a closed autoclave and subjected to heating in an oven at 170 ºC for three days. The resultant solid was filtered using vacuum

filtration and washed until a near-neutral pH was reached in the filtrate. The final product was dried in an oven at 110 ºC for 24 hours. The same procedure was repeated using a 6 M NaOH concentration, and the solid products, denoted as S5 and S6, were analyzed using Fourier Transform Infrared Spectroscopy (FTIR), X-ray diffraction (XRD), and Scanning Electron Microscopy (SEM).

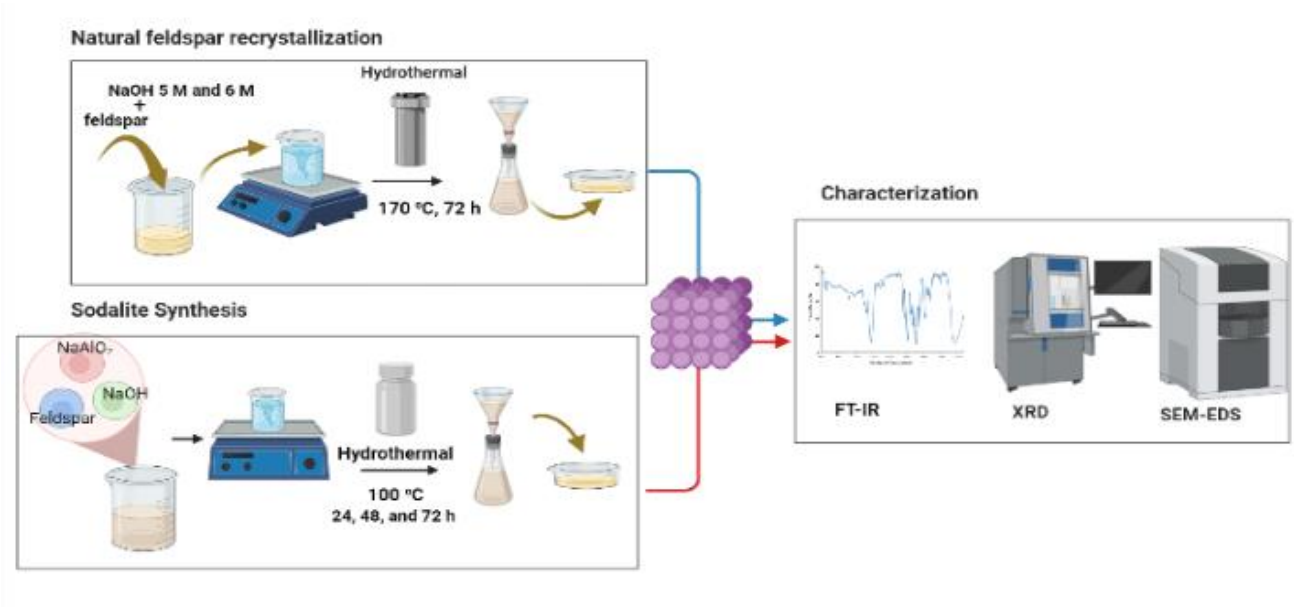

Figure 1. Schematic illustration for the preparation synthesis of SOD

The synthesis process involved dissolving 9.6 g of NaOH pellets in 149 g of distilled water in a beaker, followed by stirring until complete dissolution of the NaOH. 6.76 g of feldspar was added to the solution and stirred for 15 minutes, followed by the incorporation of 10 g of sodium aluminate. The mixture was then stirred at room temperature for 5 hours. Subsequently, the mixture was placed in a polypropylene (pp) bottle and subjected to hydrothermal treatment at 100 ºC for 24, 48, and 72 hours, respectively, and denoted as S24, S48, and S72. The resultant solid was filtered, washed with distilled water until a pH between 8-9 was reached, and dried at a temperature of 105 ºC for 24 hours. The recrystallization process uses an autoclave at a high temperature, while the SOD synthesis process uses a polypropylene bottle which is placed in an oven at a low temperature (Figure 1). The dried solid was weighed and analyzed using XRD, FTIR, and SEM-EDS analysis. Figure 1 provides a comprehensive overview of the experimental conditions utilized in the recrystallization and SOD synthesis processes.

Characterization

The XRD pattern is characterized by using X-ray diffraction (Shimadzu XRD-700 with Cu Kα radiation). Data collection was performed in the range of 2θ = 2-50 (Cu Kα). Phase identification was carried out by searching the ICDD powder diffraction database file with the aid of the IZA (zeolite database) or the Joint Committee on Powder Diffraction Standards (JCPDS) file. The FT-IR spectrum of the sample was collected by Shimadzu 8300 in the region of 4000-400 cm-1 using potassium bromide as the solvent and binder. Morphology using scanning electron microscopy (SEM-EDS -JED-2300).

RESULTS AND DISCUSSION

Synthesis of Sodalite

The recrystallization processes and synthesis processes were meticulously executed by incorporating sodium hydroxide as the mineralizing agent. The synthesis of SOD zeolite was found to be highly dependent on the dissolution gel, the number and distribution of nuclei within the prepared gel, and the rate of crystal growth during the hydrothermal treatment (Su et al., 2016). A systematic investigation was conducted to evaluate the impact of crystallization time on the formation of SOD at 100°C and the influence of NaOH concentration at 170°C. The diffraction intensity of sodalite particles was

observed to emerge after a 24-hour reaction period, implying an increase in the crystallinity of sodalite zeolite over a prolonged time.

Characterization of SOD from feldspar

The XRD analysis was performed to determine the crystallinity phase and particle size of the synthesized solid. The X-ray diffractogram of the sample at 2θ = 5°-50° is depicted in Figure 2, while the relative crystallinity and particle size values are displayed in Table 1. After synthesis under various conditions, feldspar transformed into sodalite based on the diffraction peaks at 2θ= 14.16°; 24.47°; 31.82°; 35.09°; 42.98°, by following per under crystal planes (110) (211) (310) (222) (330) and JCPDS No. 75-0709 (Arepalli et al., 2022; Kumar & Jena, 2022). X-ray diffraction results enable the determination of the crystallinity values of the synthesized solid samples. The crystallinity was calculated using Equation (1) and is presented in Table 1.

$$\%\ crystallinity = \left(\frac{\Sigma integrated\ peak\ areas\ of\ sample\ intensity}{\Sigma integrated\ peak\ areas\ of\ standard\ intensity}\right) x\ 100 \qquad (1)$$

Furthermore, the size of the crystal particles can be determined using the Scherrer equation, as expressed by Equation (2). In this equation, "d" represents the size of the crystal particles (nm), "λ" is the wavelength at 0.154 nm, "θ" is the Bragg angle, and "β" is the full width at half maximum (FWHM) of the (2 1 1) diffraction peak at 2θ = 24.65°.

$$d = \frac{0.9\ \alpha}{\beta \cos\theta} \qquad (2)$$

Table 1. The Crystallinity of the Samples as Determined from XRD Data

Sample	Crystallinity (%)	Particle size (nm)	Yield (%)
S6	90.06	21.97	87.36
S5	90.89	13.39	80.89
S72	84	14.51	88.38
S48	84	11.56	83.84
2S4	82	14.68	48,96

FTIR characterization was performed to study the bonding and molecular vibrations in solid samples synthesized with varying crystallization times and NaOH concentrations (Figure 3). The peak at 461 cm^{-1} suggests changes in Si-O bonding, while the 4-ring sodalite was seen in the 422-230 cm^{-1} range (Song et al., 2020; Su et al., 2016). The 400-800 cm-1 range is known as the fingerprint region.

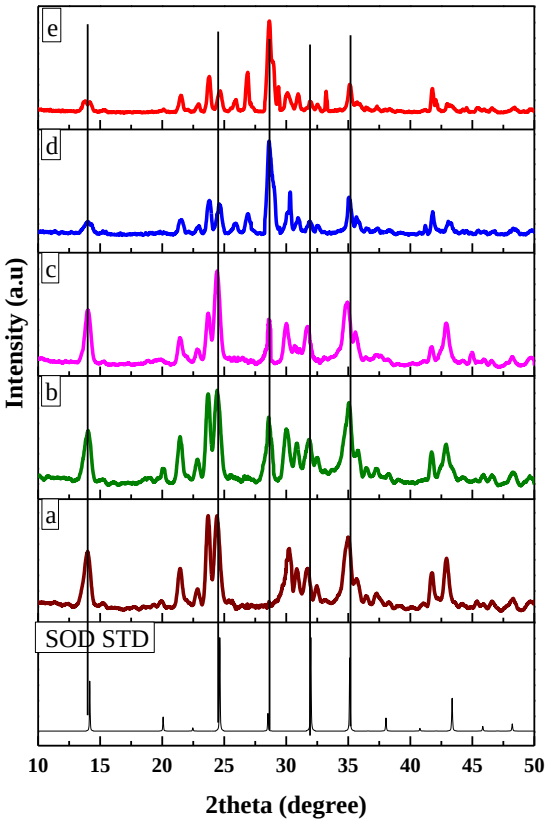

Figure 2. XRD patterns of sodalite synthesis for three days at 170˚C in NaOH solution: a. NaOH 6 M, b. NaOH 5 M; and XRD patterns of sodalite synthesis in NaOH 1,6 M solution at 100˚C after c. 72 h, d. 48 h, e. 24 h

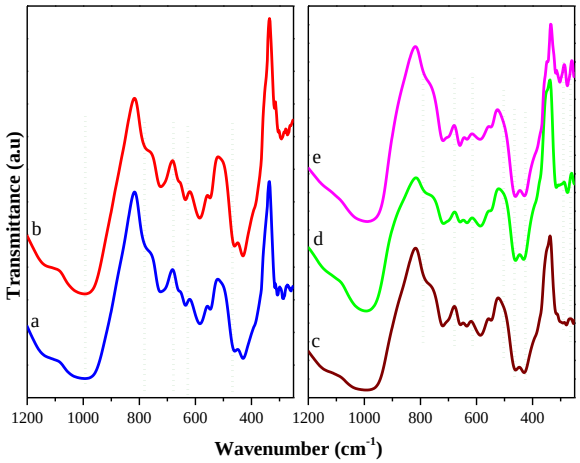

Figure 3. FTIR spectra of synthesis sodalite for 3 days at 170˚C in NaOH solution: a. NaOH 5 M, b. NaOH 6 M; and FTIR spectra of synthesis sodalite in NaOH 1,6 M solution at 100 ˚C after c. 24 h, d. 48 h, e. 72 h

The sodalite-specific peaks at 422-460 cm-1 relate to Si-O bond vibrations, and the absorption bands at 698 and 719 cm-1 correspond to Al-OH vibrations). The SOD sample shows a sodalite-specific spectrum with a peak at 987 cm-1, believed to be absorption from the asymmetric T-O-T stretch in sodalite (Ahmed et al., 2020). The peak assignments are reported in Table 2.

Table 2. Assignments of peaks observed by infrared spectroscopy of the sodalite

Samples	Asymmetric stretch [a]	Symmetric stretch [a]	Double ring	T-O band [b]
6 M	1012	631, 719	588	455, 426
5 M	993	632, 719	590	455, 426
72 h	989	657, 715	584	453, 422
48 h	993	657, 709	584	460, 430
24 h	989	651, 715	582	459, 422

[a] asymmetric stretching vibration T-O-T (T= Si/Al)
[b] < 430 cm-1 shows changes in the Si-O bond structure; > 430 cm-1 represents the bending vibrations of O-T-O and single 4-ring of sodalite (S4R).

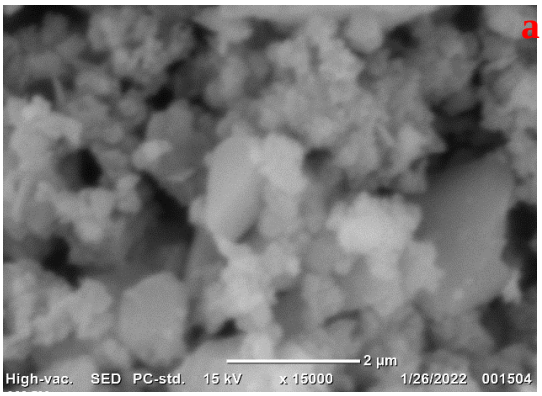

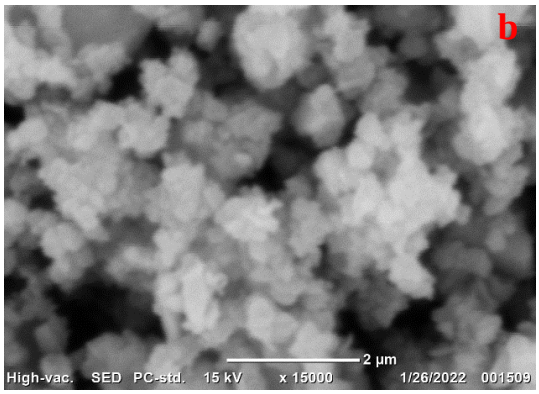

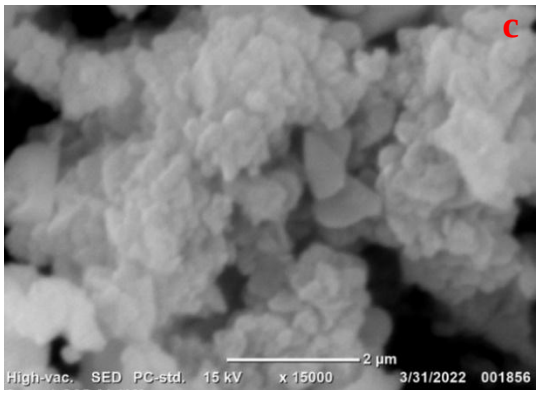

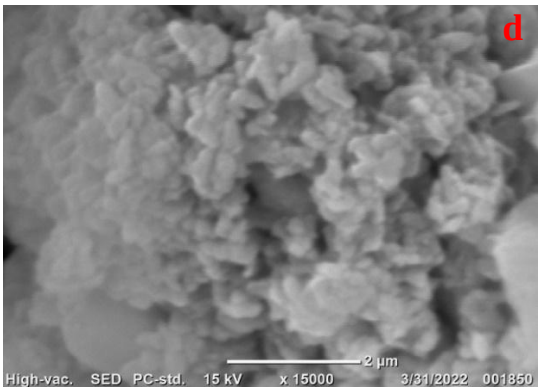

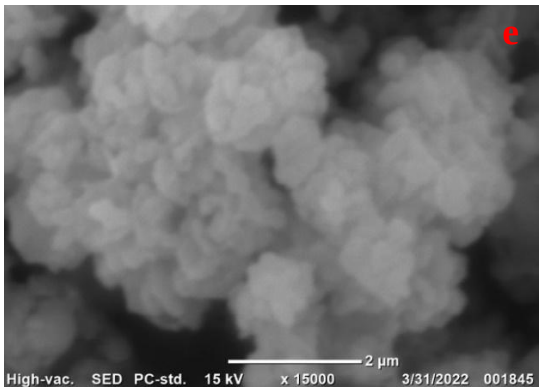

Figure 4. SEM image of recrystallization sodalite for 3 days at 170˚C in NaOH solution at 15000 times magnification: a. NaOH 5 M, b. NaOH 6 M; and SEM image of synthesis sodalite in NaOH 1,6 M solution at 100 ˚C after c. 24 h, d. 48 h, e. 72 h.

So far, the results have indicated that the SOD spectrum in the fingerprint region that was recrystallized in NaOH solution does not significantly differ from the SOD spectrum synthesized with the addition of NaAlO2. However, the presence of NaAlO2 can alter the vibrational shape and peak intensity, making them rounder in the fingerprint region. This is also supported by SEM results, which show an improved level of sodalite morphology in the NaAlO2 synthesized for 72 hours.

The mechanism of feldspar transformation into sodalite with variations in time and NaOH concentration has been found to involve a successive transformation from the amorphous phase to zeolite A, followed by transformation to sodalite. This change is associated with closer contact between the solid phase and aluminosilicate in the solution during mixing under hydrothermal conditions. The addition of aluminosilicate increases the formation of the sodalite phase (Reyes et al., 2013).

Figures 4(a-b) show Scanning Electron Microscopy (SEM) images of products synthesized with different ratios of NaOH, with S5 and S6 having aggregate morphologies of 13.39 and 21.97 nm respectively, as indicated by the SEM characterization that particle size increases with alkalinity. Figures 4(c-e) demonstrate the better morphologies of S24, S48, and S72 synthesized with variations in time and the addition of NaAlO2 to regulate the Si/Al ratio for the formation of sodalite, as shown by the SEM results with aggregate forms resembling cotton ball-like sodalite morphology. The observation of SEM images also reveals the less symmetrical form with undefined surfaces in the recrystallization results (Figures 4 a-b) compared to the more regular surfaces of the SOD synthesis results (Figures 4 c-e), which can be attributed to the significant improvement in crystal morphology due to the addition of sodium aluminate.

The results of the Energy Dispersive Spectroscopy (EDS) analysis show the distribution of elemental composition in the recrystallized and synthesized SOD (Figure 5).

The Energy Dispersive Spectroscopy (EDS) results demonstrate an increase in the Si/Al ratio as the alkalinity ratio and crystallization time increase, indicating an increase in soluble silica and alumina with increasing crystallization time.

CONCLUSION

The synthesis of sodalite from natural Indonesian feldspar using the hydrothermal method has demonstrated that the formation of zeolite crystals depends on the crystallization time and temperature. This is evidenced through chemical characteristics that show the chemical composition, size distribution, and sodalite morphology. Sodalite synthesized for 72 hours at a temperature of 100°C exhibits a better crystal form and morphology. From these characteristics, it can be concluded that the sodalite type of zeolite has the potential as a waste treatment material and catalyst support.

ACKNOWLEDGMENT

The author is grateful to the Directorate General of DIKTI-Kemendiknas through the Hasanuddin University BPPDN in 2019/2020 and the PDD Grant in 2020/2021 with contract number: 7/E1/KP.PTNBH/2021 March 8, 2021; No: 8046/UN4.1.2.3/PL.02.00/2021 March 22, 2021, No: 761/UN4.22/PT.01.03.2021 March 26, 2021.

REFERENCES

Ahmed, M. K., Afifi, M., Awwad, N. S., & Ibrahium, H. A. (2020). Pb(II) and Cd(II) removal, mechanical and morphological features of nanofibrous membranes of cellulose acetate containing fillers of hydroxyapatite, graphene oxide, and magnetite. In *Applied Physics A: Materials Science and Processing* (Vol. 126, Issue 10). Springer Science and Business Media Deutschland GmbH.

Akimkhan, A. M. (2012). Structural and ion-exchange properties of natural zeolite. *Chapter*, *10*, *261-281*.

Amin, I. I., Wahab, A. W., Mukti, R. R., & Taba, P. (2023). Synthesis and characterization of zeolite type ANA and CAN framework by hydrothermal method of Mesawa natural plagioclase feldspar. *Applied Nanoscience (Switzerland)*, *13*(8), 5389–5398. https://doi.org/10.1007/s13204-022-02756-4

An, H., Kweon, S., Park, S., Lee, J., Min, H. K., & Park, M. B. (2020). Immobilization of radioiodine via an interzeolite transformation to iodosodalite. *Nanomaterials*, *10*(11), 2157.

Arepalli, D., Rehman, A., Kim, M.-Z., Alam, S. F., & Cho, C.-H. (2022). Optimal synthesis of nanosize seeds for secondary growth of high performance hydroxy-sodalite (H-SOD) zeolite membranes for small gas and water separations. *Microporous and Mesoporous Materials*, *329*, 111451.

Flanigen, E. M., Broach, R. W., & Wilson, S. T. (2010). Zeolites in industrial separation and catalysis. *Chapter*, *1*, 1–26.

Flores, C. G., Schneider, H., Dornelles, J. S., Gomes, L. B., Marcilio, N. R., & Melo, P. J. (2021). Synthesis of potassium zeolite from rice husk ash as a silicon source. *Cleaner Engineering and Technology*, *4*, 100201.

Hamidi, R., Khoshbin, R., & Karimzadeh, R. (2021). A new approach for synthesis of well-crystallized Y zeolite from bentonite and rice husk ash used in Ni-Mo/Al2O3-Y hybrid

nanocatalyst for hydrocracking of heavy oil. *Advanced Powder Technology*, *32*(2), 524–534.

He, K., Chen, Y., Tang, Z., & Hu, Y. (2016). Removal of heavy metal ions from aqueous solution by zeolite synthesized from fly ash. *Environmental Science and Pollution Research*, *23*, 2778–2788.

Jiang, J., Gu, X., Feng, L., Duanmu, C., Jin, Y., Hu, T., & Wu, J. (2012). Controllable synthesis of sodalite submicron crystals and microspheres from palygorskite clay using a two-step approach. *Powder Technology*, *217*, 298–303.

Klima, K. M., Schollbach, K., Brouwers, H. J. H., & Yu, Q. (2022). Enhancing the thermal performance of Class F fly ash-based geopolymer by sodalite. *Construction and Building Materials*, *314*, 125574.

Kumar, M. M., & Jena, H. (2022). Direct single-step synthesis of phase pure zeolite Na–P1, hydroxy sodalite and analcime from coal fly ash and assessment of their Cs+ and Sr2+ removal efficiencies. *Microporous and Mesoporous Materials*, *333*, 111738.

Kuznetsov, P. S., Dementiev, K. I., Palankoev, T. A., Kalmykova, D. S., Malyavin, V. V., Sagaradze, A. D., & Maximov, A. L. (2021). Synthesis of highly active nanozeolites using methods of mechanical milling, recrystallization, and dealumination (A review). *Petroleum Chemistry*, *61*(6), 649-662.

Koloay, F.F.P., Sunarti, Manuhutu, J.B., (2024). Synthesis of Zeolite-A from Oil Palm Shell Ash for Adsorption of Ferrous Metal Ions in Borehole Water. *Indonesian Journal of Chemical Research*, *12*(2), 89-96.

Luo, J., Zhang, H., & Yang, J. (2016). Hydrothermal Synthesis of Sodalite on Alkali-Activated Coal Fly Ash for Removal of Lead Ions. *Procedia Environmental Sciences*, *31*, 605–614. https://doi.org/10.1016/j.proenv.2016.02.105

Ma, J., Zhang, Y., Qin, Y., Wu, Z., Wang, T., Wang, C., 2017. CunwenWang. The leaching inetics of K-feldspar in sulfuric acid with the aid of ultrasound. Ultrason. Sonochem. 35, 304–312.

Manique, M. C., Lacerda, L. V., Alves, A. K., & Bergmann, C. P. (2017). Biodiesel production using coal fly ash-derived sodalite as a heterogeneous catalyst. *Fuel*, *190*, 268-273

Ngapa, Y. D., & Ika, Y. E. (2020). Adsorpsi pewarna biru metilena dan jingga metil menggunakan adsorben Zeolit Alam Ende–Nusa Tenggara Timur (NTT). *Indonesian Journal of Chemical Research*, *8*(2), 151-158.

Pakhomova, A., Simonova, D., Koemets, I., Koemets, E., Aprilis, G., Bykov, M., ... & Dubrovinsky, L. (2020). Polymorphism of feldspars above 10 GPa. *Nature Communications*, *11*(1), 2721.

Pérez-Botella, E., Valencia, S., & Rey, F. (2022). Zeolites in adsorption processes: State of the art and future prospects. *Chemical Reviews*, *122*(24), 17647-17695

Reyes, C. A. R., Williams, C., & Alarcón, O. M. C. (2013). Nucleation and growth process of sodalite and cancrinite from kaolinite-rich clay under low-temperature hydrothermal conditions. *Materials Research*, *16*(2), 424–438. https://doi.org/10.1590/S1516-14392013005000010

Salimkhani, H., Joodi, T., Bordbar-Khiabani, A., Dizaji, A. M., Abdolalipour, B., & Azizi, A. (2020). Surface and structure characteristics of commercial K-Feldspar powders: Effects of temperature and leaching media. *Chinese Journal of Chemical Engineering*, *28*(1), 307–317.

Santoso, A., Sumari, S., Asrori, M. R., & Wele, A. R. (2024). Synthesis of Biodiesel from Refined Waste Cooking Oil with Active Natural Zeolite. *Indonesian Journal of Chemical Research*, *11*(3), 174-180.

Setiawan, I., Estiaty, L. M., Fatimah, D., Indarto, S., Lintjewas, L., Alkausar, A., ... & Jakah, J. (2020). Geologi dan Petrokimia Endapan Zeolit daerah Bayah dan Sukabumi. *RISET Geologi dan Pertambangan*, *30*(1), 39.

Song, Q., Shen, J., Yang, Y., Wang, J., Yang, Y., Sun, J., Jiang, B., & Liao, Z. (2020). Effect of temperature on the synthesis of sodalite by crystal transition process. *Microporous and Mesoporous Materials*, *292*. https://doi.org/10.1016/j.micromeso.2019.109755

Su, S., Ma, H., & Chuan, X. (2016). Hydrothermal synthesis of zeolite A from K-feldspar and its crystallization mechanism. *Advanced Powder Technology*, *27*(1), 139–144.

Wu, Y., Liu, X., Wang, Y., & Li, M. (2022). Decomposition of K-feldspar by potassium hydroxide solution in the hydrothermal system. *Minerals Engineering*, *178*, 107392.

Xu, R., Pang, W., Yu, J., Huo, Q., & Chen, J. (2009). *Chemistry of zeolites and related porous materials: synthesis and structure*. John Wiley & Sons.